Hawaiian Hot-spot Swell Structure from Seafloor MT Sounding

Steven Constable
Scripps Institution of Oceanography, UCSD, La Jolla CA 92093-0225, USA
Fax +1 858 5348090 email sconstable@ucsd.edu
(corresponding author)

Graham Heinson
Department of Geology and Geophysics, University of Adelaide, Adelaide, Australia
Fax +61 8 83034347 email Graham.Heinson@adelaide.edu.au

Manuscript for submission to *Tectonophysics* March 17, 2003

Keywords: plumes, seafloor conductivity, Hawaii swell, magnetotellurics

Abstract

Seafloor magnetotelluric (MT) data were collected at seven sites across the Hawaiian hot spot swell, spread approximately evenly between 120 and 800 km southwest of the Hawaiian-Emperor Island chain. All data are consistent with an electrical strike direction of 300°, aligned along the seamount chain, and are well fit using two dimensional (2D) inversion. The major features of the 2D electrical model are a resistive lithosphere underlain by a conductive lower mantle, and a narrow, conductive, 'plume' connecting the surface of the islands to the lower mantle. This plume is required; without it the swell bathymetry produces a large divergence of the along-strike and across-strike components of the MT fields, which is not seen in the data. The plume radius appears to be less than 100 km, and its resistivity of around 10 Ωm, extending to a depth of 150 km, is consistent with a bulk melt fraction of 5-10%.

A seismic low velocity region (LVR) observed by Laske et al. (1999) at depths centered around 60 km and extending 300 km from the islands is not reflected in our inverse model, which extends high lithospheric resistivities to the edge of the conductive plume. Forward modeling shows that resistivities in the seismic LVR can be lowered at most to 30 Ωm, suggesting a maximum of 1% connected melt and probably less. However, a model of hot subsolidus lithosphere of 100 Ωm (1450–1500°C) within the seismic LVR increasing to an off-swell resistivity of $>$1000 Ωm ($<$1300°C) fits the MT data adequately and is also consistent with the 5% drop in seismic velocities within the LVR. This suggests a 'hot, dry lithosphere' model of thermal rejuvination, or possibly underplated lithosphere depleted in volatiles due to melt extraction, either of which is derived from a relatively narrow mantle plume source of about 100 km radius. A simple thermal buoyancy calculation shows that the temperature structure implied by the electrical and seismic measurments is in quantitative agreement with the swell bathymetry.

Introduction

Two prominent features mark the passage of oceanic lithosphere over a hot-spot. The first is the initiation of oceanic volcanism leading to a chain of islands or seamounts. The second is the generation of a 1 km high, 1000 km wide bathymetric swell around the volcanic island chain. The origin of hot-spot swells is still largely unknown. At least three different mechanisms have been proposed for swell generation; (i) thermal reheating (rejuvenation) of the lithosphere within a 1000 km region centered on the hotspot (Cough, 1979; Detrick and Crough, 1978); (ii) compositional underplating of depleted mantle residue from hotspot melting (Robinson, 1988; Phipps Morgan et al., 1995); and (iii) dragging of hot plume asthenosphere by the overriding lithosphere (Sleep, 1990). The primary reason for the multiplicity of theoretical models is that there are few geophysical constraints on the structure of the lithosphere and sub-lithosphere beneath a swell (Sleep, 1990). Constraints from both global and regional seismic studies are poor, since most current global models cannot reliably resolve features of diameters less than 500 km.

The Hawaiian swell is an excellent place to study the interactions of a mantle plume with oceanic upper lithosphere due to the very high volumes of melt produced and geographic isolation from coastlines, mid-ocean ridges and subduction zones. The Hawaiian islands are almost in the center of the Pacific plate and are surrounded by lithosphere of 90-110 Ma age moving at a velocity of 83 mm.yr^{-1} (Gordon and Jurdy, 1986). In 1997, the SWELL (Seismic Wave Exploration of the Lower Lithosphere beneath the Hawaiian Swell) experiment took place, a pilot study to deploy long period hydrophones across the Hawaiian swell (Laske et al., 1999). We were able to piggyback the cruise and collect data from seven marine magnetotelluric (MT) instruments deployed in coordination with the seismic hydrophones between April and December 1997 from the RV Moana Wave. Figure 1 shows the swell (bounded by the 5000 m depth contour) and locations of MT sites (listed in Table 1). Location of sites was primarily chosen for seismic surface-wave analyses, and hence a hexagonal array with a central instrument at the ODP Borehole 843B was used (Laske et al., 1999). However, MT sites were positioned so that four MT responses were obtained above the swell (<5000 m), and three in the deeper ocean to the south of the swell, with site spacing of the order of 250 km. All instruments were successfully recovered with data.

Table 1: Instrument positions and depths.

Instrument	Latitude	Longitude	Depth	Data
Opus	19° 50.98	158° 05.43	4350 m	E/B
Noddy	19° 05.42	157° 21.53	4570 m	E/B
Lolita	17° 33.60	157° 15.60	4760 m	B
Kermit	19° 03.60	160° 26.71	4950 m	E/B
Rhonda	17° 26.98	159° 20.40	5290 m	E/B
Trevor	16° 33.63	159° 46.80	5640 m	E/B
Ulysses	15° 34.88	160° 57.05	5620 m	E/B

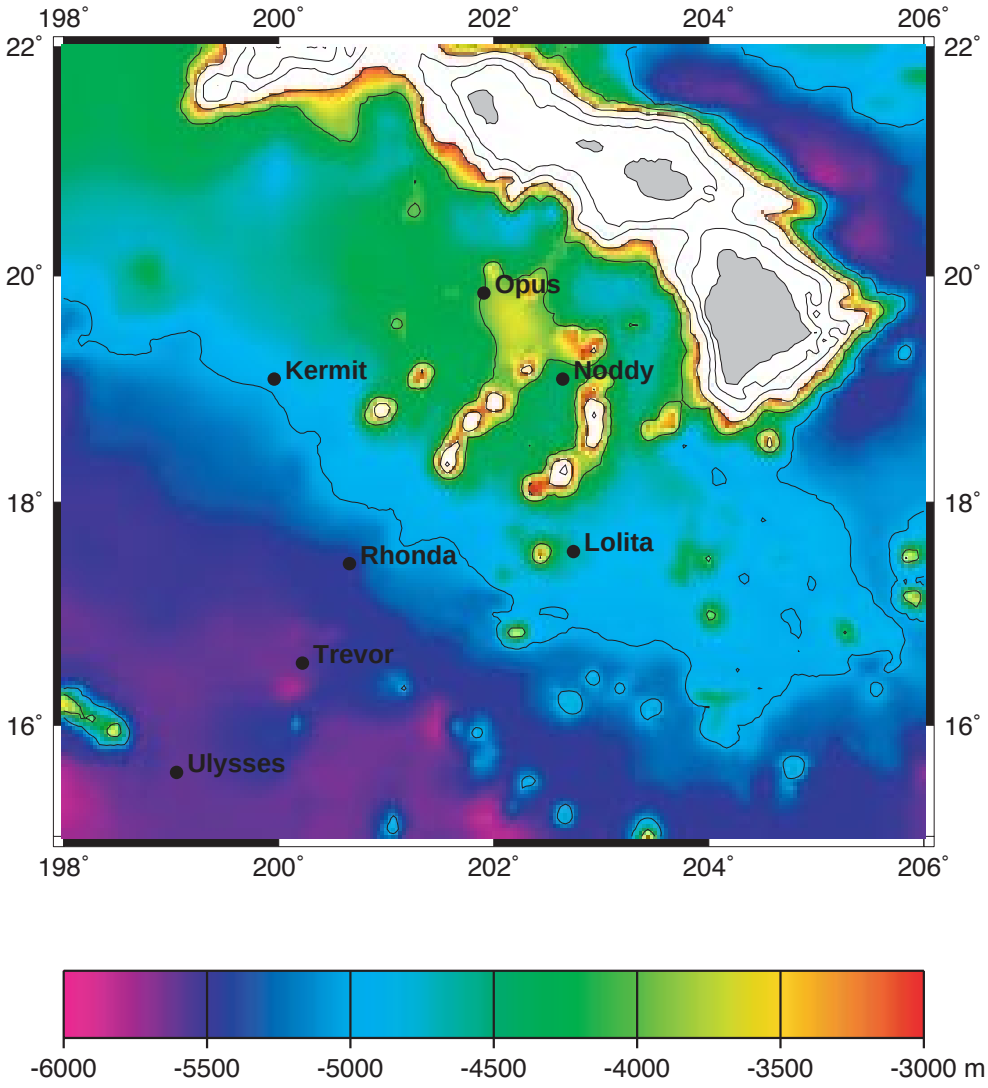

Figure 1. Location of the seven MT sites used in the experiment. All returned magnetic data, but only one channel of electric-field data was recorded at site Lolita. The edge of the swell is approximately given by the 5000 m depth contour.

Data

The MT method requires the simultaneous time-series measurement of horizontal components of magnetic (Bx and By) and electric (Ex and Ey) variational fields that result from large-scale ionospheric electric currents and temporal variations in magnetosphere morphology. Typical deep ocean MT observations are made in a bandwidth of 10^3 to 10^5 s, limited by the high electrical conductance of the ocean at short periods, and source-field non-uniformity at long periods. Short period magnetic fields are attenuated to a greater extent than electric fields because they have a higher reflection coefficient over a resistive seafloor (e.g. Constable et al., 1998). Thus the resistive nature of 100 Ma lithosphere ex-

acerbates the difficulty in recording MT fields at short periods, resulting in data with a maximum sensitivity to structure between 10 and 400 km into Earth.

Time series of eight-months duration sampled every 20 s were processed with the robust remote-reference scheme of Chave and Thomson (1989) using reference data from the shallowest sites Noddy or Opus. Site Lolita, which only recorded one channel of electric field, was processed with electric fields from site Kermit. The ratio of orthogonal horizontal components of E and B in the frequency domain is a measure of Earth's electrical resistivity at that site. With pairs of orthogonal E and B fields, MT responses may be obtained in two polarizations, or modes. Above 1D layered structures the two MT modes are identical, but for 2D structures MT fields may be rotated to modes of electric field parallel to strike (TE mode) and perpendicular to strike (TM mode). More complex 3D structures will have non-uniform MT responses that cannot be simply decomposed to TE and TM modes. The ratio of vertical magnetic field (Bz) to the horizontal fields (Bx and By), known as GDS, or tipper, responses, also provides a measure of lateral changes in resistivity. If no lateral changes exist, Bz will be zero for periods in the bandwidths stated above. Typical processing errors are less than 5% in the bandwidth 10^3 – 4×10^4 s, and 10% or greater at shorter or longer periods.

Distortion effects were analyzed using the methods of Groom and Bailey (1989) and the Mohr circle method of Lilley (1998). Azimuths were found to be generally independent of period, at $61\pm10^\circ$ west of geographic north. Thus, induction (and galvanic current flow) is predominantly 2D at all MT sites, with an azimuth orientated parallel to the strike of the 5000 m contour (edge of the swell in Figure 1), and the islands. At each site, the MT fields were rotated to the dominant 2D azimuth determined by decomposition, and we define the TE mode to be parallel to edge of the swell, and the TM mode to be perpendicular. Apparent resistivities are smaller in the TM mode, particularly at sites closest to the islands, as might be expected from the classical geomagnetic coast (or island) effect. Figure 2 shows data pseudo-sections of all data, and Figure 3 shows MT responses at sites Opus and Ulysses, the shallowest/easternmost and deepest/westernmost sites respectively. For Opus, there is a clear DC-offset in apparent resistivity between the two modes, suggestive of a galvanic static-shift effect. However, it is presumably difficult to maintain the near-surface charge buildup necessary for a true static-shift in the presence of uniformly conductive seawater, and Opus phases are also different at all periods, suggesting inductive, rather than galvanic, effects. More likely, it is the effect of the islands and bathymetry that accounts for the anisotropy between modes; data from Ulysses, furthest from the islands, are more isotropic, particularly at long periods.

The TM mode resistivity is most obviously influenced by the islands' geomagnetic coast-effect, increasing in resistivity with distance. At distances greater than 600 km, TE and TM modes are almost equal, indicating an approximately 1D response. On the other hand, TE apparent resistivities, much less affected by the island bathymetry, are higher for the sites on the swell, and reduce significantly off-swell. A similar response can be seen in the GDS tipper values in Figure 3. The largest response in the real (in-phase) tippers is at the edge of the swell (about 400 km from the islands), and surprisingly small close to the islands where a larger response might be expected. Tippers of 0.4 or more are very large considering the

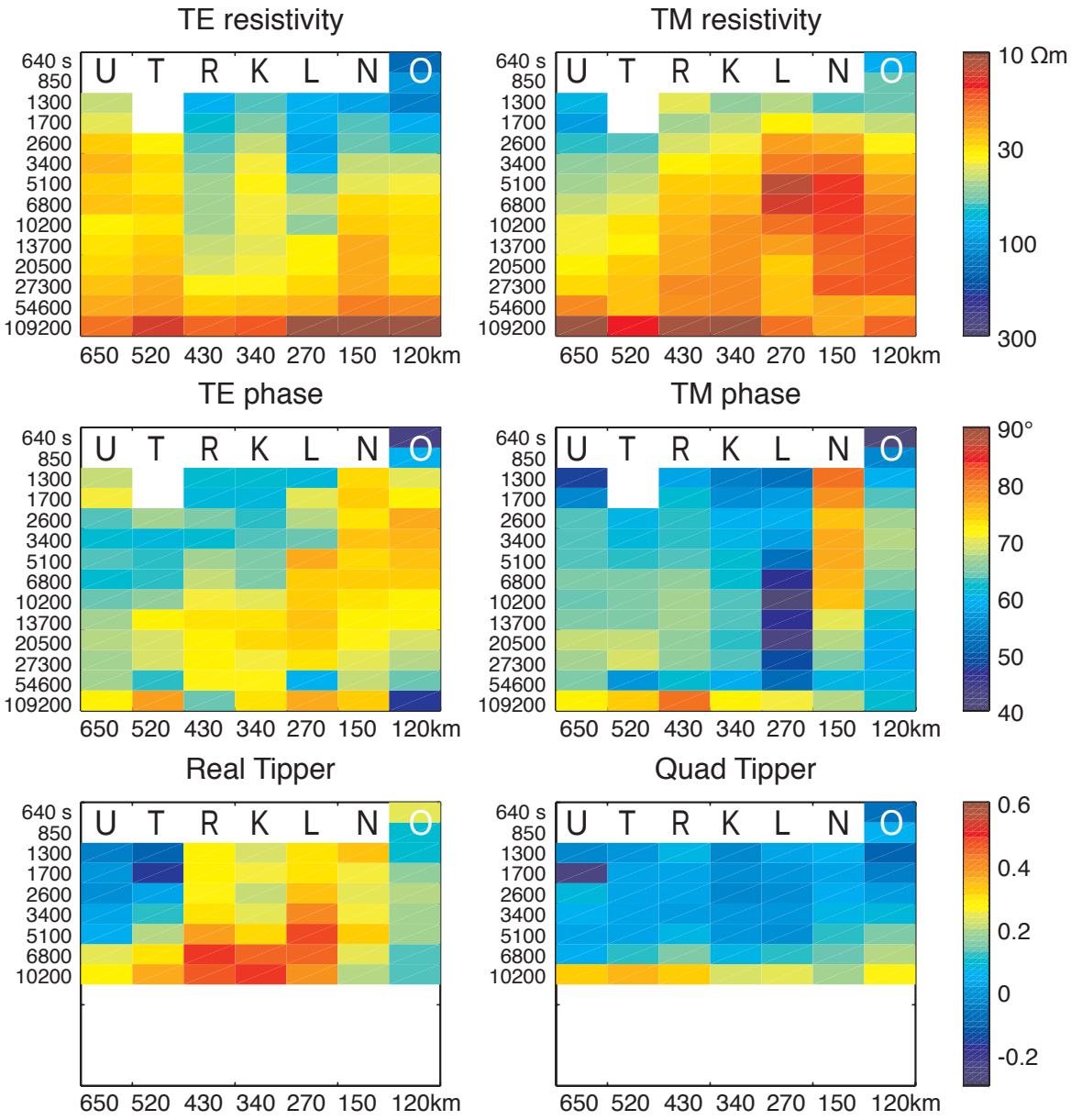

Figure 2. Data pseudo-sections (log period vs. approximate distance west from island chain) of MT and GDS data at all sites. MT data are shown as apparent resistivity and phases, in TE (electric field parallel to island chain) and TM (electric field perpendicular). GDS tippers responses are shown for real (in-phase) and quadrature (out-of-phase) components. The edge of the swell is about 400 km from the island chain.

shallow seafloor gradients (about 1% in Figure 1) and the relatively small lateral and vertical size of the islands compared to the depth of the ocean. Quadrature (out-of-phase) tippers show a more uniform response, changing sign from negative to positive at about 6×10^3 s period at all sites, and are generally much smaller than the real tippers. Figure 4 shows real and quadrature Parkinson induction arrows at four periods superimposed on island and seafloor topography. All real arrows are orientated approximately perpendicular to the swell topography and towards the deep ocean. At periods longer than 10^4 s, quadrature arrows are similar in amplitude ($\approx$0.3) and all orientated towards the southwest. The explanation for such behaviour is not clear. One possible reason is source-field inhomogenieties, but

the latitude of the experiment (16-20° N) is well away from the geomagnetic electrojet that would otherwise cause such effects. Alternatively, ocean basin scale coast-effect may be responsible (Heinson and Constable, 1992).

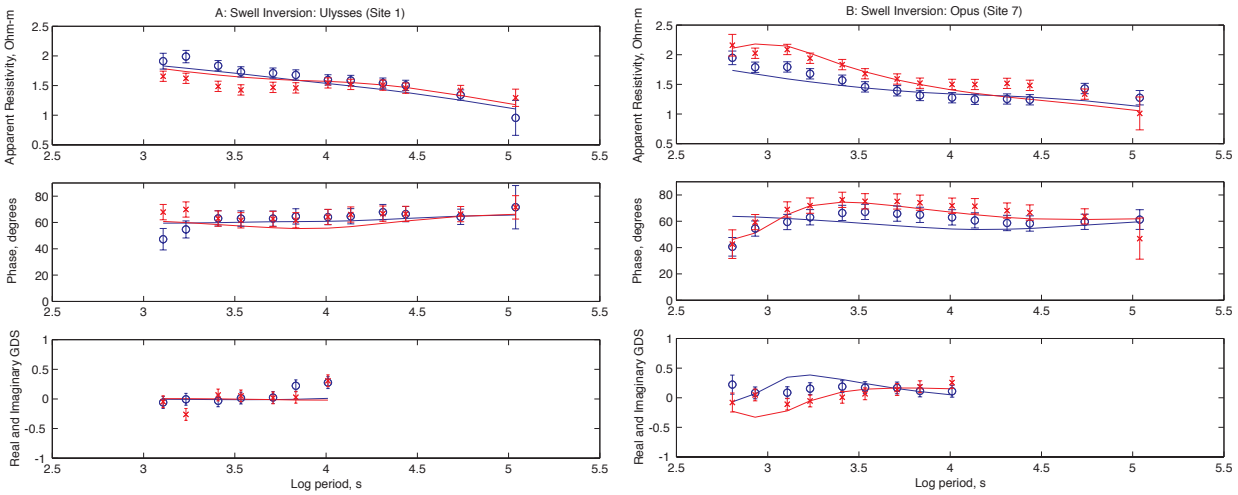

Figure 3. MT response curves from Opus and Ulysses. For each site, the two modes are TE shown by red 'x' (electric fields parallel to bathymetry and island chain) and TM shown by blue 'o' (elecric fields perpendicular). For the GDS data, the real component is shown as blue 'o', and the quadrature (imaginary) component by red 'x'. Solid lines represent the resonse of the 2D inversion shown in Figure 5. Data are shown with one standard deviation error bars for a 20% error floor in resistivity.

Inversion

Although MT sites are located at various distance and azimuth from the active volcanism of the islands, the orientation of the swell is approximately 2D and parallel to the direction of spreading. Thus, a 2D Occam's inversion (deGroot-Hedlin and Constable, 1990) of the sites was carried out as a function of distance from the island chain. Seabed topography was included as a discrete set of topographic ramps of 200 m separated by 100 km, exploiting the triangular elements of Wannamaker et al.'s (1986) finite element forward code used by the inversion. The island chain is represented by a 150 km wide block that comes within 300 m of the sea-surface. Approximating topography and sites to mesh nodes was not simple, as clearly the sites are not orientated along a single line. Local topographic variations (such as the seamounts close to site Noddy) were not included. The plume is undoubtedly 3D, but as the plume-width is probably of the order of 100 km, and the nearest sites (Opus and Noddy) are some distance away, we can justify the 2D approach. (Simpson et al. (2000) considered the dimensionality of a possible plume by analyzing daily variations in the magnetic field at two islands, but such sparse data lack the ability quantify lateral extent.) Small errors produced by the response function estimation procedure were removed by creating a noise floor of 20% error in resistivity, 5.8° in phase, and 0.1 in GDS data. The maximally smooth Occam inversion was able to fit the entire data set (both modes of resistivity, phase, and GDS) to rms = 1.35. Figure 5 shows a smooth resistivity model fitting the data to rms = 1.4, and Figure 3 shows examples of the fits of this model to the two data sets at the extremes of

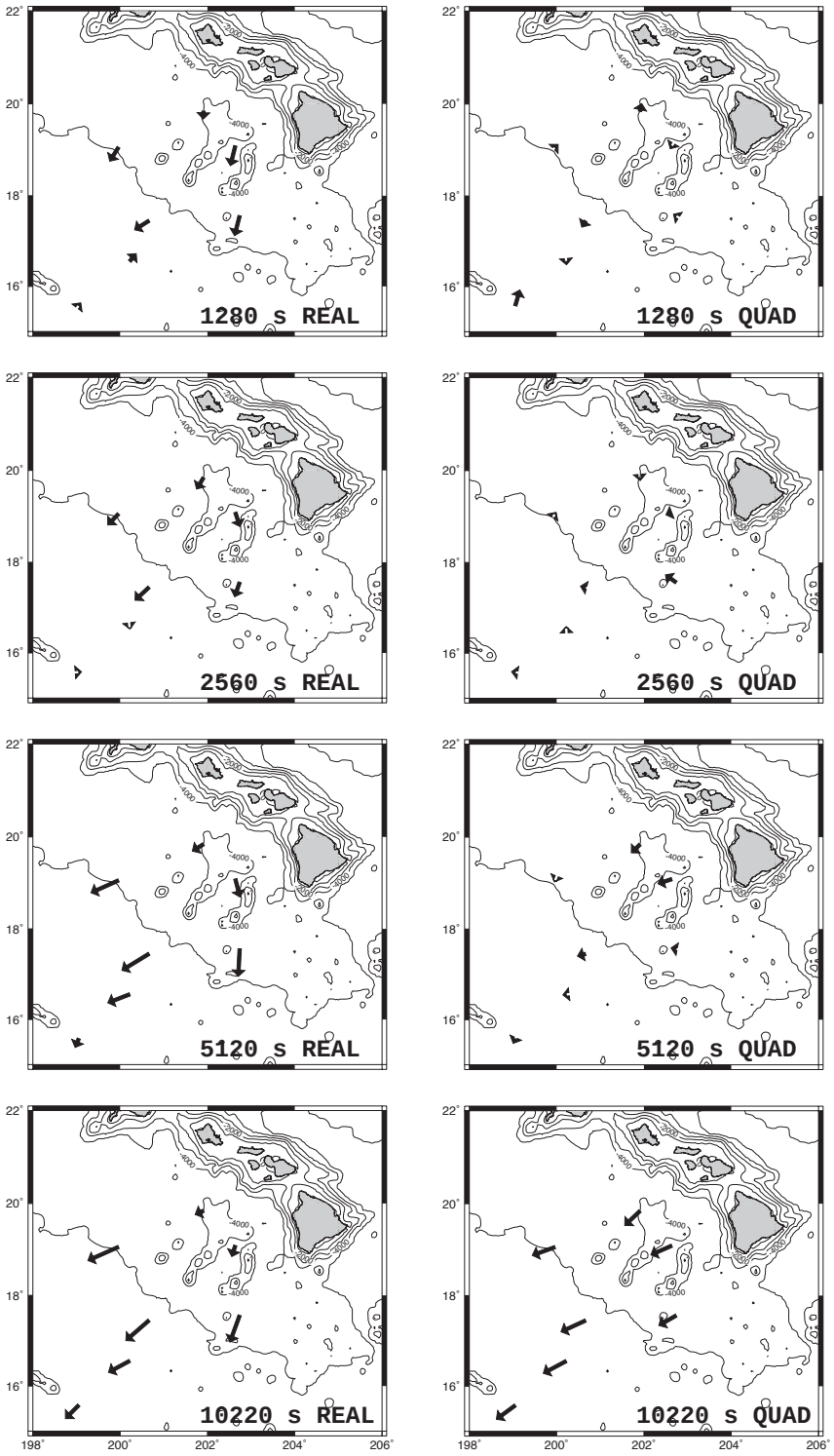

Figure 4. Parkinson real and quadrature arrows plotted on a map of seafloor topography at four periods of induction. The largest arrows are about 0.6– see Figure 2 for quantitative data.

the profile, Ulysses to the west and off the swell, and Opus at the base of the island chain. We see more anisotropy in the MT response (a difference between the TE and TM modes) close to the islands, but not as much as one would expect from such topography. Fits to the

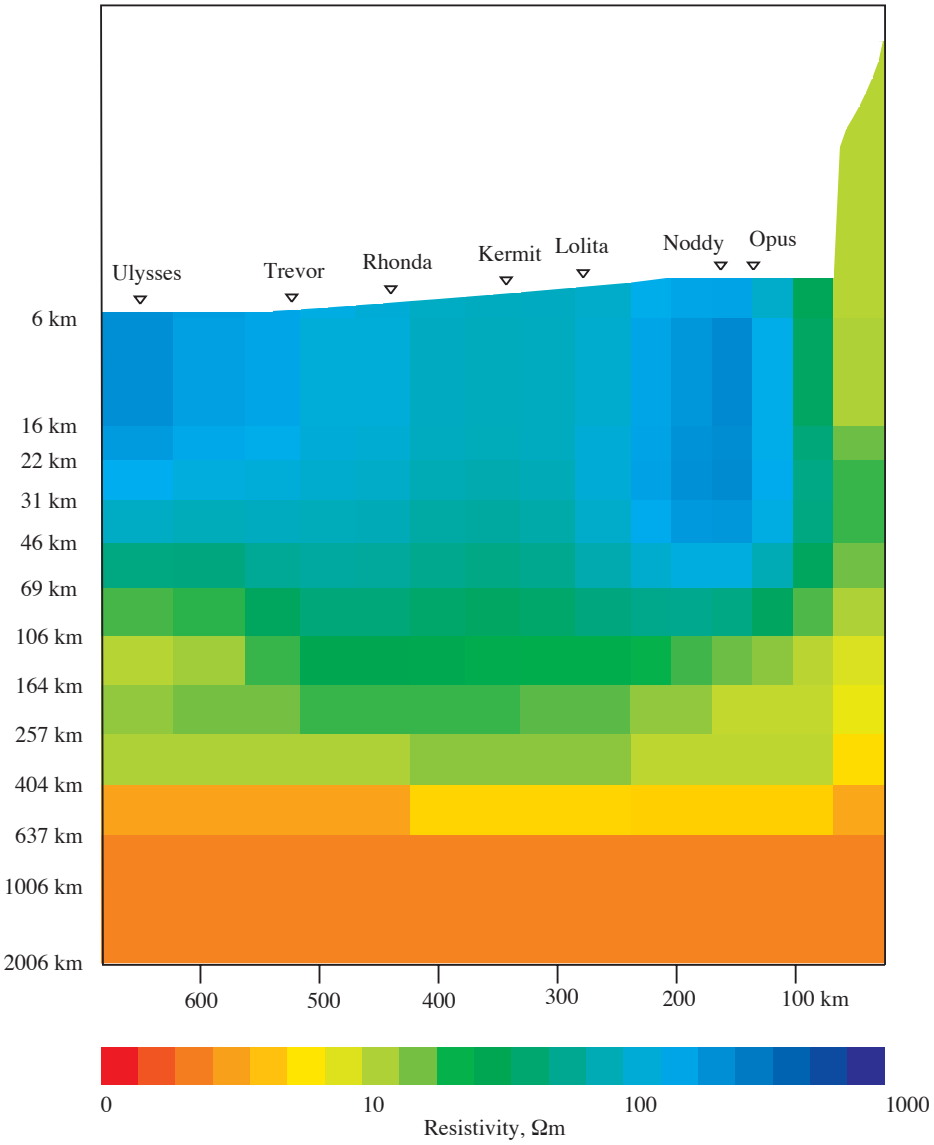

Figure 5. Two-dimensional smooth inversion of MT and GDS data from the six marine sites. The island chain is represented by a ridge coming to within 300 m of the sea surface, and the model east of the islands is terminated with seawater layer (not shown here).

other four data sets are qualitatively similar.

The model in Figure 5 shows a suprising uniformity in resistivity across the swell. The dominant features of the model are an increase in conductivity with depth at around 400–1000 km, well known from analysis of long period magnetic observatory data and associated with the phase changes in olivine in the upper mantle and to perovskite/magnesiowustite in the lower mantle (e.g. Xu et al., 2000), and increased conductivity immediately below the island chain, suggestive of a combination of high temperatures, melt, and seawater-filled porosity (i.e., a mantle plume and associated surface volcanism). To a depth of 100 km away from the islands, the lithosphere is relatively uniform at $\approx$100 Ωm. The resistivity of this

lithospheric layer is almost certainly underestimated, because MT has poor sensitivity to resistive layers embedded in conductive structure (represented here by the oceans and lower mantle). We note that this layer derives from depleted mantle at mid-ocean ridges, and hence is probably mostly anhydrous. Constable and Cox (1996) argue, based on their controlled source EM experiments, that at least 10^4 Ωm is typical for cool, olivine-rich lithosphere at temperatures less than 600° C, well below the mantle solidus. The MT method, on the other hand, can only quantify the resistivity of such features by means of vertical TM mode current flow, forced by lateral conductivity contrasts such as coastlines. However, in this case the islands lack a strong TM response as a result of their low resistivity.

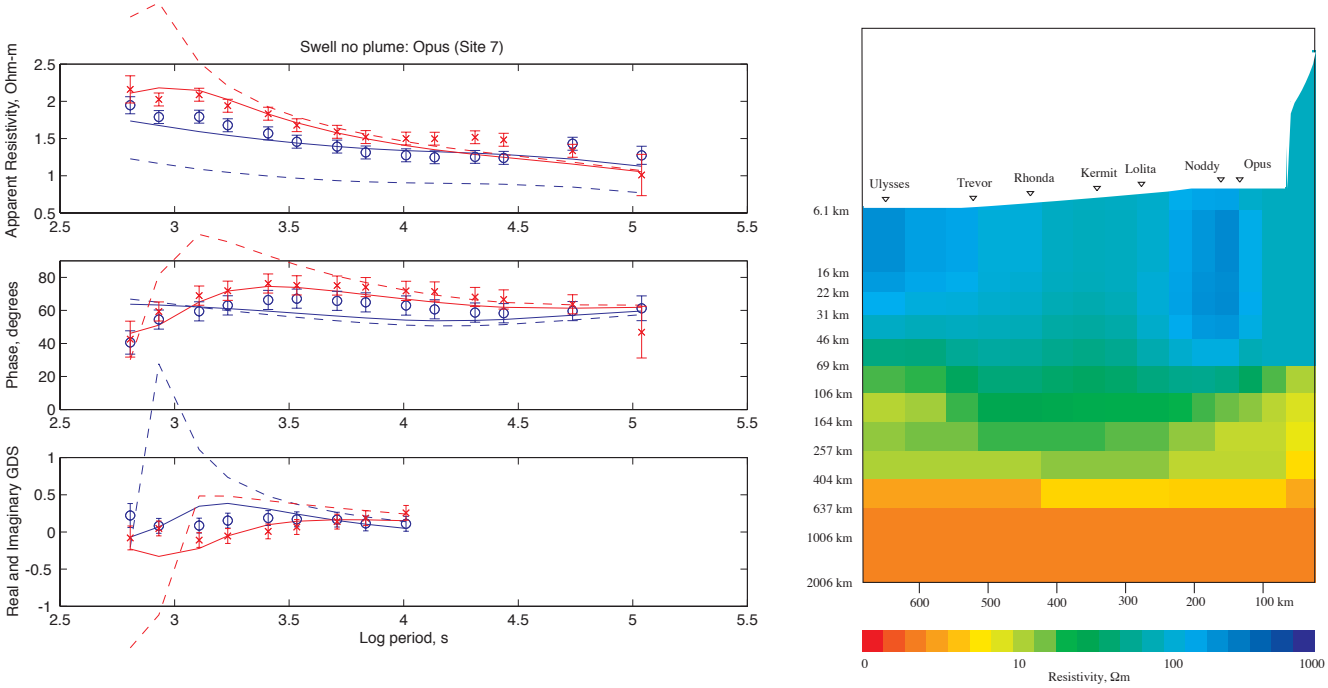

Figure 6. Model in which the conductive plume is removed from the inverted model (right) and the fit to the nearest site, Opus (broken lines in left plot). Solid lines on the data plot show the fits of the unperturbed inversion model of Figure 5. It can be seen that the fit to the data is completely corrupted, providing a great deal of confidence in the existence of the electrical plume.

Forward Modeling

While the inversion produces a good fit to the data, forward models are used to test the necessity of features in the inverse model, and compatibility with other geophysical data.

Requirement for a plume

We are not the first to suggest an electrically conductive plume beneath Hawaii. An inversion of land MT and GDS data from Oahu in the period range 10^4 – 10^7 s by Larson (1975) and

Neal et al. (2000) showed similar resistivities to our model; 1–10 Ωm to depths of 700 km. Simpson et al. (2000) also find evidence for lower resistivities beneath the island of Hawaii where volcanism is current, but their analysis has almost no lateral resolution; our study is the first to provide measurement sites with a significant lateral extent, allowing the size of the plume to be estimated.

Although our model exhibits evidence for a high conductivity plume beneath the islands, it is relatively narrow (only 100 km or so) and off to the side of our array. It is therefore prudent to test whether it is in fact required by the data, and a forward model was run in which the low resistivities beneath the islands were replaced by 100 Ωm material to a depth of 70 km. This model increases the data misfit to rms = 2.55 overall, and, as shown in Figure 6, the misfit to the station closest to the islands is particularly unacceptable.

Compatibility with the seismic model

Laske et al. (1999), on analysing surface wave seismic data from the SWELL experiment, find a region of slower shear-wave velocities centred around 70 km depth and extending over 300 km from the islands. Our inversion shows no evidence of this feature in the resistivity data, and indeed this region is the most resistive part of the model. This increased resistivity is likely a result of better quality high frequency data from the instruments in shallower water than a real feature of the lithosphere, but nevertheless the implication is that the lower seismic velocities do not result from partial melting, which would increase conductivities dramatically. To test how conductive this region could be made without compromising data fits, a decreased resistivity region was included where the seismic shear wave velocities were below 4.3 m/s (Figure 7). Any decrease in the resistivity of this region below 100 Ωm degrades the fit to the data; by the time the resistivity is reduced to 30 Ωm the fits are significantly poorer (rms = 1.58). A further decrease in resistivity to 10 Ωm produces an unambiguous misfit (rms = 2.35), exemplified in Figure 7 for site Opus.

Thermal anomaly

If not partial melt, then perhaps a thermal anomaly causes the low seismic velocities beneath the swell. Our lithospheric resistivities of 100–300 Ωm are consistent with an essentially dry olivine rock of 1400 – 1500 °C (Figure 9). Although these resistivities extend to the southwestern edge of the model, we do not expect the entire lithosphere to have this temperature and resistivity. We know that normal oceanic lithosphere is much more resistive than 100 Ωm (Constable and Cox, 1996), and we have already noted that the seafloor MT method is not sensitive to such highly resistive structure. We thus tested the model shown in Figure 8, maintaining a resistivity of 100 Ωm within the seismic LVZ, and increasing the lithospheric resistivity outside the LVZ to 1000 Ωm. The thickness of this electrical lithosphere is set at 60 km, based on the controlled source EM work of Constable and Cox (1996). We have, of course, maintained the electrical plume necessary to preserve the data fits.

The statistical misfit associated with this model is rms=1.58, a small but nevertheless significant decrease in acceptability. However, the fit to our benchmark site in shallow water, shown in Figure 8, is still qualitatively good and in some respects might be considered better

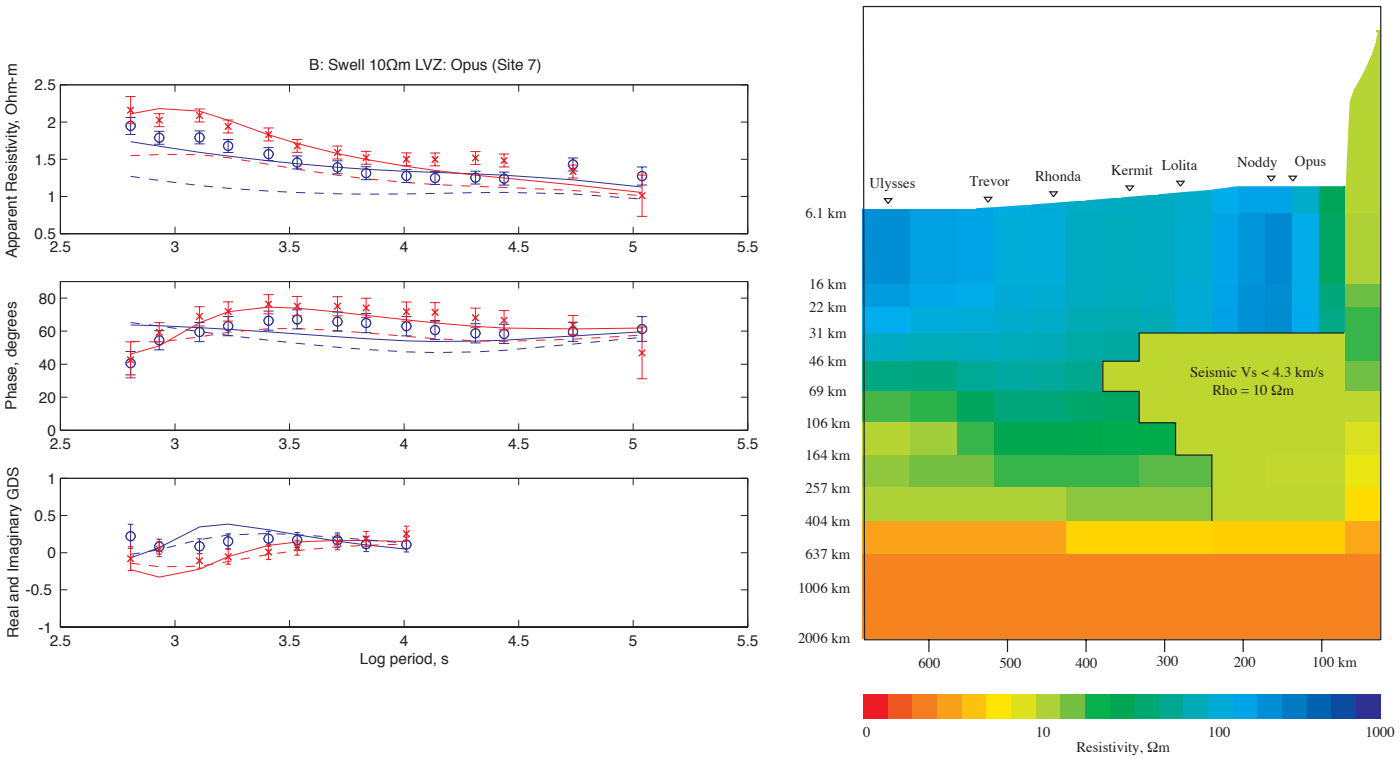

Figure 7. Model in which the region with lower seismic shear wave velocity (less than 4.3 m/s) is replaced by resistivities of 10 Ωm (right) and fits to the nearest site, Opus (left). Solid lines show the response of the inversion model of Figure 5, while broken lines show the response of the modified model. Although the effect is not as dramatic as removing the plume, this modification of the inverse model also ruins the fit to the data.

than the smooth inversion. One could expect that small adjustments to the geometry of our thermal model could restore the data misfit while preserving the underlying concept of a hot, dry swell anomaly surrounded by normal lithosphere.

Table 2: Thermal buoyancy calculation.

Model Depth, km	Δ depth	Geotherm, °C	Δ T, °C	β, m
31 – 46	15	500	900	405
46 – 69	23	800	600	414
69 – 106	37	1100	300	333
106 – 164	58	1300	100	174
			total	1326

Discussion

In our efforts to explain the origin of the Hawaiian swell, it is natural to ask if the thermal anomaly represented by Figure 8 is consistent with observed bathymetry. Taking the simple

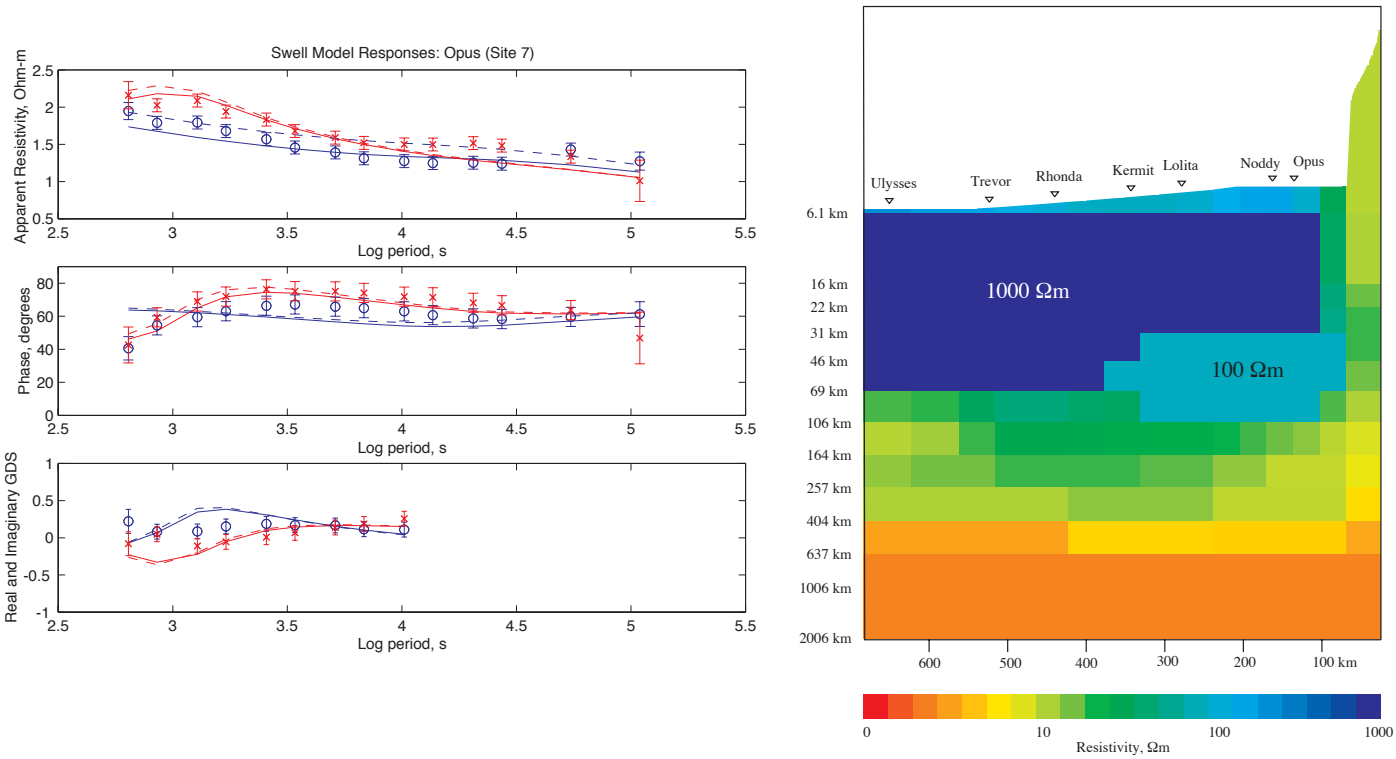

Figure 8. Model (right) in which the region with lower seismic shear wave velocity (less than 4.3 m/s) is maintained at 100 Ωm while the resistivity of the surrounding lithosphere is increased to 1000 Ωm, representing a thermal anomaly associated with the LVZ. The data misfit associated with this model is, from a statistical sense, a barely acceptable 1.58, but as can be seen from site Opus (left), provides a good qualitative fit to the data.

model of Sleep (1990), thermally supported bathymetry is given by

$$\beta = \Delta d.\Delta T.\alpha$$

where Δd is thickness of the thermal layer supporting the bathymetry, ΔT is the temperature anomaly, and α is the thermal expansion coefficient of the mantle, which here we take to be that of olivine, or approximately 3×10^{-5} C^{-1} (Ribe and Christensen, 2001). If we take the temperature inside our thermal anomaly to be 1400 °C, and the temperature of the surrounding lithosphere to be given by an oceanic geotherm appropriate for 90 My age, then Table 2 provides estimates of ΔT, Δd and β for each layer of the resistivity model between 31 km, where the anomaly starts, and 164 km where the temperature in the anomaly reaches that of the geotherm. If we sum the cumulative effects, we arrive at a total buoyant bathymetry of 1326 m, which agrees well with the difference in depth of our deepest and shallowest instruments (1270 m, Table 1).

High resistivity in the uppermost 50 km suggests uniform temperature gradients across the swell, consistent with seafloor heat-flow measurements that show little variation with location (von Herzen et al., 1982; 1989). Therefore, as for the seismic surface-wave analyses of Laske et al. (1999), the resistivity model does not support the concept of lithosphere thinning

and reheating as proposed by Detrick and Crough (1978). Below the swell, resistivity is of order 100 Ωm or higher to depths of 60–160 km. A similar structure was determined beneath the Society Islands hot-spot by Nolasco et al. (1998). Plume temperatures are estimated to be 1500°C at a depth of 100 km, and the excess temperature of the asthenosphere beneath the swell (assumed to be 100 km thick) is predicted to be 200 to 300°C (Sleep, 1990). A high temperature asthenosphere over depths of 60 to 160 km beneath the swell is supported by seismic surface-wave analyses (Laske et al., 1999).

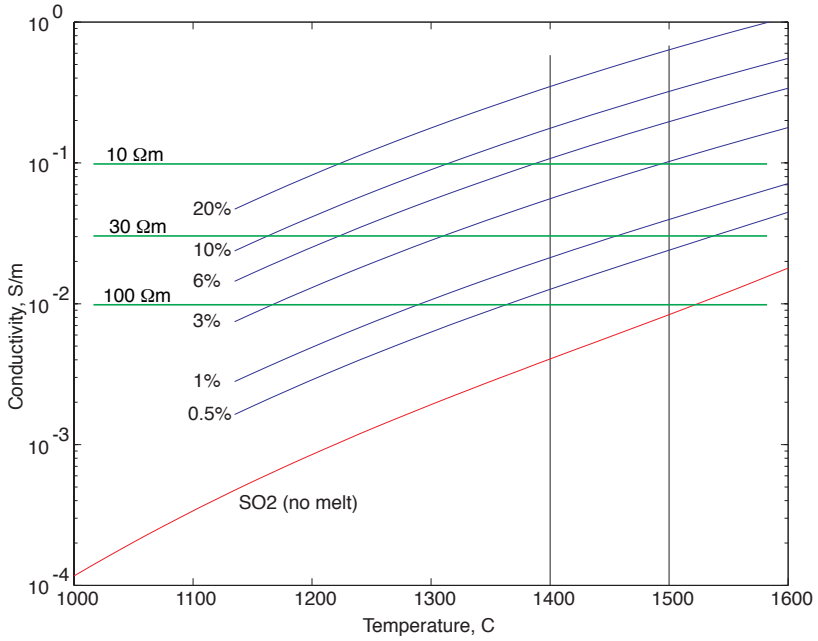

Figure 9. Predictions for mantle conductivity based on measurements of subsolidus olivine by Constable et al. (1992) and melt by Tyburczy and Waff (1983), using a binary mixing model of well-connected melt along grain-edge tubes.

Forward modeling shows that the region of seismic low velocities cannot have a resistivity much lower than 100 Ωm, and can in fact be significantly more resistive. This sub-swell asthenospheric resistivity is consistent with laboratory measurements on olivine (SO2 model) between 1400 to 1500°C (Constable et al., 1992) and the thermal models of Heinson and Constable (1992) for 100 Ma seafloor. Even at the lower bounds of permissible resistivity, this region is permeated by at most 1% connected partial melt: Figure 9 shows predictions for mantle conductivities as a function of temperature and melt content using the SO2 model of Constable et al. (1992) for subsolidus olivine, and melt conductivities from Tyburczy and Waff (1983) (see also Roberts and Tyburczy, 1999). Conductivities resulting from mixing the two phases were predicted using the tube model of Grant and West (1965), which approximately represents well-connected melt along grain edges. We see that 100 Ωm mantle between 1400 and 1500°C is at the solidus, with at most 0.5% connected melt. Allowing the region of lower seismic velocities to be 30 Ωm only increases the possible connected melt content to 1%. To explain the 5% anomaly in seismic velocities observed by Laske et

al. (1999) in terms of partial melt would require melt fractions of 3-4% (Sato et al., 1989), which is unlikely given the high resistivities observed in this region; 3% melt would require 10 Ωm in the seismic low velocity region, which we have already shown to be incompatible with the MT data. However, again appealing to Sato et al. (1989), seismic velocities decrease 5% as the temperature is increased from about 0.9 to 1.0 times the melting temperature. This corresponds to about 200 K, which, with reference to Figure 9, corresponds to about an order of magnitude in electrical conductivity, and is suggestive of an off-swell lithosphere of 1250°C or lower with resistivities of 1000 Ωm or higher, and a region corresponding to reduced seismic velocities which is at 1450°C or higher with a resistivity of around 100 Ωm. We ran such a forward model, and the fits to the data are indeed acceptable (rms = 1.58).

Beneath the islands, our 2D and Larsen's (1975) 1D inversions show a low resistivity (around 10 Ωm) structure in the top 150 km of the plume. Assuming that the plume beneath Hawaii has a core temperature of between 1300-1500°C, then sub-solidus olivine conduction cannot explain the observed resistivities. An obvious candidate for reduced resistivities is the presence of melt at depths of up to 120 km. A melt fraction of 7% (White and McKenzie, 1995) implies a bulk resistivity of around 10 Ωm (Figure 9), in good agreement with our results. Melt connection beneath Hawaii may be anisotropic, with higher vertical than horizontal conductivities, but there are too few data to pursue this problem at present. Above the seafloor, the islands also have low resistivity, perhaps due to high porosity filled with hot saline fluids.

Acknowledgments. We would like to thank the officers and crew of the RV Moana Wave for two excellent cruises in April and December, 1997. A. White, J. Phipps Morgan, G. Laske, L. MacGregor and K. Key contributed to various aspects of deployments and recoveries. At Flinders University, A. White, B. Perkins and B. Walker, and at Scripps Institution J. Lemire and T. Deaton are thanked for support equipment design and construction. G. Heinson was funded by the Australian Research Council. Funding under the National Science Foundation grant number OCE 95-29707 provided logistical support for the MT deployments.

References

Chave, A.D. and Thomson, D.J., 1989. Some comments on magnetotelluric response function estimation, J. Geophys. Res., 94, 14,215-14,225.

Constable, S.C. and Cox, C. S., 1996. Marine controlled source electromagnetic sounding 2. The PEGASUS experiment, J. Geophys. Res., 101, 5,519-5,530.

Constable, S.C., Shankland, T.J. and Duba, A., 1992. The electrical conductivity of an isotropic olivine mantle. J. Geophys. Res., 97, 3,397-3,404.

Constable, S.C., Orange, A.S., Hoverston, M.G. and Morrison, F.H., 1998. Marine magnetotellurics for petroleum exploration, part 1: A seafloor equipment system, Geophysics, 63, 816-825.

Crough, S.T., 1978. Thermal origin of mid-plate hot-spot swells, Geophys. J. R. astr. Soc., 55, 451-469.

deGroot-Hedlin, C. and Constable, S.C., 1990. Occam's inversion to generate smooth two-dimensional models from magnetotelluric data, Geophysics, 55, 1,613-1,624.

Detrick, R.S. and Crough, S.T., 1978. Island subsidence, hot spot, and lithosphere thinning, J. Geophys. Res., 97, 2,037-2,070.

Gordon, R.G. and Jurdy, D.M., 1986. Cenozoic global plate motions, J. Geophys. Res., 91, 12,389-12,406.

Grant, F.S. and West, G.F., 1965. Interpretation Theory in Applied Geophysics, McGraw-Hill, New York.

Groom, R W. and R.C. Bailey, 1989. Decomposition of magnetotelluric impedance tensors in the presence of local three-dimensional galvanic distortion, J. Geophys. Res., 94, 1,193-1,925.

Heinson, G.S. and Constable, S.C., 1992. The electrical conductivity of the oceanic upper mantle, Geophys. J. Int., 110, 159-179.

Larsen, J.C., 1975. Low frequency (0.1 - 6.0 cpd) electromagnetic study of deep mantle electrical conductivity beneath the Hawaiian islands, Geophys. J. R. astr. Soc., 43, 17-46.

Laske, G., Phipp Morgan, J. and Orcutt, J.A., 1999. First results from the Hawaiian SWELL experiment, Geophys. Res. Lett., 26, 3,397-3,400.

Lilley, F. E. M., 1998. Magnetotelluric tensor decomposition: Part I, Theory for a basic procedure, Geophysics, 63, 1,885-1,897.

Nolasco, R., Tarits, P., Filloux, J.H. and Chave, A.D.: 1998. Magnetotelluric imaging of the Society Islands Hot Spot, J. Geophys. Res., 103, 30287-30309.

Neal, S.L., Mackie, R.L., Larsen, J.C. and Schultz, A., 2000. Variations in the electrical conductivity of the upper mantle beaneath North America and the Pacific Ocean, J. Geophys. Res., 105, 8,229-8,242.

Phipps Morgan, J., Morgan, W.J. and Price, E., 1995. Hotspot melting generates both hotspot volcanism and a hotspot swell?, J. Geophys. Res., 100, 8,045-8,062.

Ribe, N.M. and Christensen, U.R., 1999. The dynamical origin of Hawaiian volcanism, Earth Planet. Sci. Lett., 171, 517-531.

Roberts, J.J. and Tyburczy, J.A., 1999. Partial-melt electrical conductivity: Influence of melt composition J. Geophys. Res., 104, 7,055-7,065.

Robinson, E.M., 1988. The topographic and gravitational expression of density anomalies due to melt extraction in the uppermost oceanic upper mantle, Earth Planet. Sci. Lett., 90, 221-228.

Sato, H., Sacks, I.S., and Murase. T., 1989. The use of laboratory velocity data for estimating temperature and partial melt fraction in the low-velocity zone: comparison with heat flow and electrical conductivity studies, J. Geophys. Res., 94, 5,689-5,704.

Simpson, F., Stevelimg, E. and Leven, M., 2000, The effect of the Hawaiian plume on the magnetic daily variation, Geophys. Res. Lett., 27, 1,775-1,778.

Sleep, N.H., 1990. Hotspots and mantle plumes: some phenomenology, J. Geophys. Res., 95, 6,715-6,736.

Tzyburcy, J.A., and Waff, H.S., 1983. Electrical conductivity of molten basalt and andesite to 25 kilobars pressure: geophysical significance and implications for charge transport and melt structure, J. Geophys. Res., 88, 2,413-2,430.

von Herzen, R.P., Detrick, R.S., Crough, S.T., Epp, D. and Fehn, U., 1982. Thermal origin of the Hawaiian swell: Heat flow evidence and thermal models, J. Geophys. Res., 87, 6,711-6,723.

von Herzen, R.P., Cordery, M.J., Fang, C., Detrcik, R.S. and Fang, C., 1989. Heat flow and the thermal origin of hot spot swells: The Hawaiian swell revisited, J. Geophys. Res., 94, 13,783-13,800.

Wannamaker, P.E., Stodt, J.A., and Rijo, L., 1986. A stable finite element solution for two-dimensional magnetotelluric modelling, Geophys. J. R. astr. Soc., 88, 277-296.

White, R.S. and McKenzie, D.P., 1995. Mantle plumes and flood basalts, J. Geophys. Res., 100, 17,543-17,585.

Xu, Y.S., Shankland, T.J., and Poe B.T., 2000. Laboratory-based electrical conductivity in the Earth's mantle J. Geophys. Res., 105, 27,865-27,875.